



1 **Significant secondary formation of nitrogenous organic aerosols in an urban atmosphere revealed by**
2 **bihourly measurements of bulk organic nitrogen and comprehensive molecular markers**

3
4 Xu Yu¹, Min Zhou², Shuhui Zhu², Liping Qiao², Jinjian Li³, Yingge Ma², Zijing Zhang¹, Kezheng Liao³,
5 Hongli Wang², Jian Zhen Yu^{1,3,4,*}

6
7 ¹Division of Environment and Sustainability, Hong Kong University of Science & Technology, Clear Water
8 Bay, Kowloon, Hong Kong, China

9 ²Key Laboratory of Formation and Prevention of Urban Air Pollution Complex, Ministry of Ecology and
10 Environment, Shanghai Academy of Environmental Sciences, Shanghai, China

11 ³Department of Chemistry, Hong Kong University of Science & Technology, Clear Water Bay, Kowloon,
12 Hong Kong, China

13 ⁴Fok Ying Tung Graduate Research Institute, Hong Kong University of Science & Technology, Nanshan,
14 Guangzhou, China

15
16 Corresponding author: jian.yu@ust.hk

17
18
19 **Key points:**

20 1. Various primary and secondary sources of aerosol organic nitrogen (ON) have been quantitatively resolved
21 using PMF model based on bihourly measurement data of bulk ON and comprehensive source markers

22
23 2. Observational evidence of formation of reduced ON species through ammonia chemistry was found

24
25 3. Joint source analyses of ON and organic carbon (OC) facilitated investigating the potentially significant
26 formation pathways of ON aerosols

27



28 **Abstract**

29 Nitrogenous organic aerosol (OA) has a significant impact on solar radiation, human health, and ecosystems.
30 However, our knowledge of the total budget of aerosol organic nitrogen (ON) and its major sources,
31 particularly the secondary formation processes, remains largely qualitative. In this study, we conducted
32 bihourly measurements of aerosol ON and a comprehensive array of organic and inorganic source markers
33 in urban Shanghai during the fall-winter period of 2021. ON accounted for 6-58% of the total aerosol N,
34 averaging 20%. Positive factorization matrix source apportionment revealed that both primary emissions
35 (52%) and secondary formations (48%) made substantial contributions to the ON mass. Dominant primary
36 ON sources included coal combustion and vehicle emissions, accounting for 21% each. Five significant
37 secondary formation processes involving ON formation were identified, namely nitrate formation (14%),
38 photochemical formation (10%), nitroaromatics formation (7%), dicarboxylic acids (DCA) formation (8%),
39 and oxygenated cooking OA (7%). DCA formation-related ON likely represented reduced N-containing
40 organic species such as imidazoles and amides. Nitrate formation processes produced OA with a very low
41 organic carbon-to-ON ratio, suggesting a heterogeneous/aqueous formation of organic nitrates. Our field
42 work provides first quantitative source analysis and new insights into the secondary formation processes of
43 ON aerosols in an urban atmosphere.

44

45 **Key words**

46 Nitrogenous organic aerosol; Secondary formation processes; Bulk organic nitrogen; Source apportionment



47 **1 Introduction**

48 Nitrogen (N)-containing organic compounds are significant constituents of ambient organic aerosols (Yu et al., 2024), and their environmental effects have been observed in various aspects. For example, nitroaromatic
49 compounds (Laskin et al., 2015; Xie et al., 2017) and imidazole-like species (Bones et al., 2010; Li et al.,
50 2019) are typical brown carbon molecules that absorb solar radiation, leading to a warming effect. Amines
51 are more efficient than ammonia (NH₃) in reacting with sulfuric acid to form new particles (Qiu et al., 2011),
52 even in urban regions with high aerosol loading (Yao et al., 2018). Nitro-polycyclic aromatic hydrocarbons
53 (nitro-PAHs) are known toxicants to the human body (Miller-Schulze et al., 2010; Bandowe et al., 2017).
54 Additionally, the atmospheric deposition of organic nitrogen (ON) species serves as a significant source of
55 N nutrient for marine and remote continental regions (Kielland et al., 2006; Andersen et al., 2017; Li et al.,
56 2023). Therefore, detailed investigations are warranted to understand the budgets and sources of ON aerosols
57 considering their multiple important environmental effects.

58
59 Several compound categories of ON have been identified, including urea (Mace et al., 2003; Violaki and
60 Mihalopoulos, 2011), amino acids (Zhang et al., 2002; Ren et al., 2018), amines (Ho et al., 2016; Liu et al.,
61 2018a), N-heterocyclics (Samy and Hays, 2013; Rizwan Khan et al., 2017), nitroaromatics (Chow et al., 2016;
62 Xie et al., 2017), nitro-PAHs (Wei et al., 2012), and organic nitrates (Li et al., 2018; Huang et al., 2021b).
63 While urea stands as a single compound, several to dozens of individual compounds have been quantified in
64 each of the other categories. Despite considerable quantification uncertainty, aerosol mass spectrometry
65 (AMS) has been widely used to estimate the total amount of organic nitrates (Farmer et al., 2010; Huang et
66 al., 2021b; Xu et al., 2021). Overall, the quantifiable individual ON species or a specific ON category
67 commonly constitute only a minor fraction of the total ON aerosol content (Jickells et al., 2013). The
68 comprehensive quantification of every ON molecule to derive the total ON aerosol budget is impractical due
69 to the lack of knowledge of molecular composition of the ON fraction and standards. Alternatively, bulk ON
70 measurement, though lacking detailed compositional data, enables mass closure and aids in exploring major
71 sources of ON aerosol. Traditional methods of aerosol ON quantification have relied on the difference
72 method, where ON is calculated as the difference between total nitrogen (TN) and inorganic nitrogen (IN)
73 (Cape et al., 2011). Limitations with the traditional analytical approach for aerosol ON determination have
74 led to three deficiencies in the current status of aerosol ON data.

75 First, the assessment of aerosol total ON, including both water-soluble ON (WSON) and water-insoluble
76 ON (WION), has been quite restricted, with most determinations focusing solely on water-soluble TN
77 (WSTN), omitting WION measurements (Cape et al., 2011). This approach produces WSON through taking
78 the difference between WSTN and IN. Some studies have employed elemental analyzers for TN
79 determination, calculating ON as the difference between TN and IN (Duan et al., 2009; Miyazaki et al., 2011;
80 Pavuluri et al., 2015; Matsumoto et al., 2019). However, the elemental analyzers' detection limit of nitrogen
81 is insufficient for accurate measurements of trace-level aerosol nitrogen (Duan et al., 2009), limiting its
82 widespread use in aerosol nitrogen analysis. Despite significant uncertainty, a few studies suggested that
83 WION, deduced by subtracting WSTN from TN, could be more abundant than WSON in coastal or urban
84 areas (Pavuluri et al., 2015; Matsumoto et al., 2019), highlighting the necessity of quantifying total ON to



85 determine the extent of ON aerosol presence. Second, the quantification of both WSON and WION using
86 the difference method introduces considerable uncertainty, especially when ON is a minor fraction of TN
87 (Yu et al., 2021). This approach has led to the reporting of physically implausible negative WSON
88 concentrations in past studies (Mace et al., 2003; Nakamura et al., 2006; Violaki and Mihalopoulos, 2010; Yu
89 et al., 2017). Third, absence of high-time resolution or online measurement methods for aerosol ON has
90 hampered the investigation of ON aerosol sources and formation processes in previous research.

91 We have developed an analyzer system that utilizes programmed thermal evolution of carbonaceous and
92 nitrogenous aerosols and chemiluminescence detection coupled with multivariate curve resolution data
93 treatment (Yu et al., 2021). This system enables simultaneous quantification of aerosol IN and ON with high
94 sensitivity and accuracy. Unlike conventional methods, our new approach avoids the occurrence of negative
95 ON concentrations, which are often encountered in difference methods. Furthermore, the method allows for
96 both offline and online measurements of aerosol ON. During the summer of 2021, we conducted a two-
97 month period of online observations of aerosol IN and ON in urban Shanghai (Yu et al., 2023). Our findings
98 revealed significant diurnal variations in ON concentrations, with vehicle emissions and secondary
99 formation processes identified as major drivers of episodic ON enhancements. However, due to the lack of
100 comprehensive organic source markers, we were unable to fully attribute the contributions of certain
101 potentially important sources and/or formation processes to the ON budget.

102 In this study, we extended our investigation through online measurements of aerosol ON in urban
103 Shanghai during the fall-winter period of 2021. Concurrently, we conducted comprehensive measurements
104 of aerosol major components and source markers on an hourly/bihourly scale. Specifically, we measured a
105 comprehensive array of organic tracers representing distinct primary emission sources and secondary
106 formation processes. These measurements enabled us to quantitatively apportion total ON to different
107 primary and secondary sources using positive matrix factorization (PMF) receptor modeling. Our focus lies
108 in examining the secondary formation sources of ON, as our knowledge regarding the formation mechanisms
109 of ON aerosols remains limited. By combining the high-time resolution measurements of ON and
110 comprehensive organic markers, we demonstrate the successful quantitative source analysis of ON aerosols
111 in an urban atmosphere, revealing significant contributions of secondary formation pathways to ON.

112

113 **2 Methodology**

114 **2.1 Sampling site and period**

115 The field measurement was conducted in Shanghai, a megacity located in the Yangzi River Delta (YRD)
116 region of China and with a population of over 24 million. In recent years, the city has experienced frequent
117 episodes of PM_{2.5} pollution, with nitrogenous components becoming increasingly prominent contributors to
118 PM_{2.5} mass (Zhou et al., 2022). All measurements were carried out at a monitoring site (31.17°N, 121.43°E)
119 situated on the rooftop of an eight-story building, approximately 30 meters above the ground, at the Shanghai
120 Academy of Environmental Sciences (SAES). This site is surrounded by urban roads, commercial activities,
121 and residential dwellings, making it a representative urban location influenced by a diverse range of emission
122 sources (Wang et al., 2018; Zhou et al., 2022). The observations were conducted during the fall-winter period



123 from November 6 to December 31, 2021.

124 **2.2 Online measurement of aerosol ON**

125 Aerosol ON was measured bihourly using our newly developed analytical system, which enables sensitive
126 and simultaneous measurements of aerosol ON and IN. Detailed descriptions of the new method can be
127 found in our previous work (Yu et al., 2021; Yu et al., 2023). In brief, the analyzer system integrates two
128 commercial instruments: an online aerosol carbon (C) analyzer and a chemiluminescence NO_x analyzer.
129 Carbonaceous and nitrogenous aerosols collected on quartz filters are thermally evolved under programmed
130 temperatures and then catalytically oxidized to CO₂ and nitrogen oxides (NO_y), respectively. The C signal is
131 monitored using the non-dispersive infrared (NDIR) method, while the N signal is recorded through
132 chemiluminescence detection after converting NO_y to NO. The C signal assists in differentiating IN and ON
133 components since ON aerosols produce both C and N signals, while the IN fraction only gives an N signal.
134 The programmed thermal evolution facilitates the separation of aerosol IN and ON, as they exhibit distinct
135 thermal characteristics. The quantification of IN and ON is achieved through multivariate curve resolution
136 data treatment of C and N thermal fractions (Yu et al., 2021).

137 The time resolution for ON measurement is 2 hours, with each sampling lasting one hour, followed by an
138 analysis step taking around 50 minutes. Sampling commenced at even hours (e.g., 02:00, 04:00). In total,
139 598 pairs of available ON and IN data points were collected. 4-methyl-imidazole was used as the standard
140 for calibrating C and N measurements, with calibration performed twice a month. The detection limit for
141 aerosol N is 0.013 µgN, corresponding to an air concentration of 0.027 µgN m⁻³.

142 **2.3 Other online measurements**

143 The measurement methods for PM_{2.5} mass and major aerosol components at the site have been described in
144 detail elsewhere (Qiao et al., 2014). PM_{2.5} concentration was measured using a beta attenuation particulate
145 monitor (Thermo Fisher Scientific, FH 62 C14 series). Organic and elemental carbon (OC and EC) were
146 monitored using a semicontinuous OC/EC analyzer (model RT-4, Sunset Laboratory, Tigard, OR, USA). The
147 major water-soluble ionic species (NO₃⁻, Cl⁻, SO₄²⁻, Na⁺, NH₄⁺, K⁺, Mg²⁺, and Ca²⁺) in PM_{2.5} were measured
148 using the Monitor for Aerosols and Gases (MARGA) (ADI, 2080; Applikon Analytical B.V.). Elements in
149 PM_{2.5} (e.g., Al, K, Ca, Mn, Fe, Ni, Cu, Zn, As, Se, Cd, Pb) were monitored using an online x-ray fluorescence
150 (XRF) spectrometer (Xact® 625, Cooper Environmental Services, Tigard, OR, USA). All the instruments
151 were equipped with individual sampling inlets with a cyclone to achieve a 2.5 µm cut size. The sampling
152 lines, made of stainless steel, were approximately 2-2.5 m in length.

153 Quantification of a suite of speciated organic markers was conducted using a Thermal desorption Aerosol
154 Ggas chromatography–mass spectrometer (TAG, Aerodyne Research Inc.). The measurement principle and
155 operational procedure of the TAG system have been described in detail in previous studies (Williams et al.,
156 2006; He et al., 2020; Zhu et al., 2021). In brief, the TAG system operated at a time resolution of 2 hours.
157 During the first hour, ambient air was drawn through a PM_{2.5} cyclone at a flow rate of 10 L min⁻¹, passing
158 through a carbon denuder to remove the gas phase, and particles were then collected onto a thermal
159 desorption cell (CTD). In the second hour, the collected particles underwent thermal desorption and gas
160 chromatography–mass spectrometry (GC-MS) analysis. In each analysis, 5 µL of an internal standard



161 mixture was added to the CTD that was loaded with particles collected in the preceding hour. During the
162 thermal desorption step, the polar organic compounds in the PM_{2.5} were derivatized to their trimethylsilyl
163 derivatives under a helium stream saturated with the derivatization agent N-methyl-N-(trimethylsilyl)
164 trifluoroacetamide (MSTFA). Subsequently, the organic compounds were reconcentrated onto a focusing
165 trap cooled by a fan. Following this, the CTD was purged with pure helium to remove excess MSTFA, and
166 the focusing trap was heated to 330°C to transfer the organic compounds into the valveless injection system,
167 which utilizes a restrictive capillary tube to connect to the GC inlet. The GC-MS analysis was then initiated.
168 A total of around 100 polar and nonpolar organic compounds could be identified and quantified with
169 authentic standards (Zhu et al., 2023). The individual TAG-measured source tracers used for PMF receptor
170 modeling are listed in Table S1.

171 Gaseous pollutants, including sulfur dioxide (SO₂), ozone (O₃), nitrogen dioxide (NO₂), nitric oxide (NO),
172 and carbon monoxide (CO), along with meteorological parameters such as temperature, relative humidity,
173 atmospheric pressure, visibility, wind speed, and wind direction, were also recorded. The trace gas and
174 meteorological data were averaged to an hourly resolution to match the time resolution of other analyses.

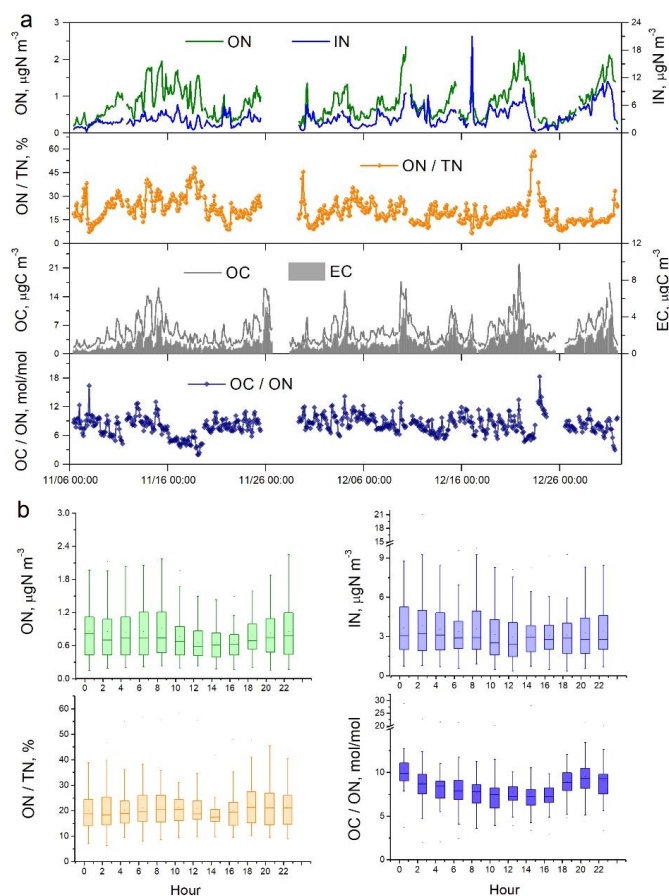
175

176 **3 Results and discussion**

177 **3.1 Abundance and variations of ON aerosol.**

178 The concentration of aerosol ON ranged from 0.15 to 2.35 μgN m⁻³, with the average being 0.80±0.45 μgN
179 m⁻³ during the fall-winter period of observation (Figure 1). IN concentration was on average 3.34±2.16 μgN
180 m⁻³ and displayed a large variation from 0.34 to 21.05 μgN m⁻³. ON accounted for 6-58% of the total N in
181 aerosols, with an average of approximately 20%. This percentage was significantly lower than ($p < 0.001$)
182 the value (25%) observed at the same location during the summer of 2021 (Yu et al., 2023). The difference
183 was attributed to the higher enhancement of IN (2.2 times) compared to ON (1.8 times) from summer to
184 winter. During the winter observation, ON exhibited significantly higher concentrations at nighttime (0.85
185 μgN m⁻³) compared to daytime (0.75 μgN m⁻³) ($p < 0.005$) (Figure 1). This result contradicted the findings
186 from summertime measurements, which showed higher ON concentrations during daytime (Yu et al., 2023).
187 From summer to winter, the daytime and nighttime ON concentrations increased by a factor of 1.56 and 2.13,
188 respectively, suggesting that nocturnal formation of ON aerosols might be more significant in winter. The
189 concentration of aerosol IN was significantly higher during nighttime in both summer and winter periods at
190 the urban site.

191 The average of OC/ON atomic ratio was 8.15, with an interquartile range of 6.92 to 9.34 during the fall-
192 winter observation (Figure 1). That is, in most cases there was one N atom relative to 7-9 C atoms in the
193 collected organic aerosols. The average of OC/ON atomic ratio was significantly lower in winter than in
194 summer (8.15 vs 11.98) ($p < 0.001$). Since the major primary sources of OC and ON did not change much
195 at the urban site over seasons, which is discussed below, the lower OC/ON ratio suggested that during
196 wintertime, when air pollution is more severe, more N element was incorporated into organic molecules to
197 form secondary N-containing OA. Therefore, detailed investigations into the sources, particularly the
198 secondary formation processes of nitrogenous OA, are warranted.



199

200 **Figure 1.** (a) Time series of aerosol N and C concentrations as well as ON/TN and OC/ON ratios during the
 201 fall-winter field observations in urban Shanghai from November 06 to December 31 of 2021. The OC/ON
 202 values are atomic ratios, calculated by measured OC/ON mass ratios divided by (12/14). (b) Diel variations
 203 of ON and IN concentrations as well as ON/TN and OC/ON ratios.
 204

205 3.2 Source apportionment for aerosol ON by PMF model with comprehensive source markers.

206 In this study, bihourly measurements of aerosol total ON together with a comprehensive list of organic and
 207 inorganic source markers were available. This allows us to quantitatively resolve the various sources of ON
 208 using PMF receptor modeling. The diel variations of ON sources can be revealed from the model results.
 209 The descriptions of PMF run are provided in Text S1 in Supporting Information. Benefiting from the
 210 comprehensive array of molecular source tracers, the PMF analysis resolved a total of 18 factors, including
 211 8 primary emission sources and 10 secondary formation sources. The factor profiles and contributions are
 212 displayed in Figure S2 and Figure S3, respectively. The 18 factors were identified by the characteristic tracers
 213 in individual source profiles (Qiao et al., 2014; Wang et al., 2015), which were: (1) manganese (Mn), iron (Fe),
 214 and zinc (Zn) for industrial emissions; (2) selenium (Se), and lead (Pb) for coal combustion; (3) levoglucosan,
 215 mannosan, and galactosan for biomass burning; (4) hopanes, NO_x , and EC for vehicle emissions; (5) nickel



216 (Ni) for ship emissions; (6) saturated and unsaturated fatty acids for cooking emissions; (7) azelaic acid, 9-
217 oxononanoic acid, and nonanoic acid for oxygenated cooking OA formation. This factor shows the profile
218 of oxidation products from cooking emissions. It could be found that both cooking emissions and oxygenated
219 cooking OA showed significantly enhanced contributions during dinner time (Figure S3b); (8) sodium (Na^+)
220 and chloride (Cl^-) for sea salt emissions; (9) silicon (Si) and calcium (Ca) for soil dust; (10) nitrocatechols
221 for nitrocatechol formation processes. Nitrocatechols are a combination of 4-nitrocatechol, 3-methyl-5-
222 nitrocatechol, and 4-methyl-5-nitrocatechol. These species were significantly correlated with each other,
223 with R-squared values ranging from 0.4 to 0.8; (11) 4-nitrophenol for nitrophenol formation processes. Note
224 that nitroaromatic compounds are notable constituents of nitrogen-containing OA, which leads us to include
225 nitrocatechols and nitrophenol in the PMF analysis to resolve ON fraction linking with nitroaromatic
226 components; (12) nitrate (NO_3^-) for nitrate formation processes; (13) sulfate (SO_4^{2-}) for sulfate formation
227 processes; (14) O_3 for photochemical formation processes; (15) phthalic acid for phthalic acid formation
228 processes; (16) dicarboxylic acids (DCAs) for DCA formation processes; (17) isoprene and α -pinene SOA
229 tracers for isoprene & α -pinene SOA formation processes; and (18) β -caryophyllenic acid for β -
230 caryophyllene SOA formation processes. The 18-factor solution exhibited excellent agreement with the
231 observed ON and OC masses (Figure S4). 12 out of the 18 factors have contributed to the ON mass, while
232 no ON was distributed in the remaining 6 factors including biomass burning, ship emission, sea salt emission,
233 sulfate formation, phthalic acid formation, and isoprene & α -pinene SOA formation processes.

234 Overall, 52% ($0.42 \mu\text{gN m}^{-3}$) of the ON mass was derived from primary emissions (Figure 2). Coal
235 combustion and vehicle emissions were the two dominant primary sources of ON, each contributing
236 approximately 20% to the aerosol ON. This finding was consistent with the summertime measurements at
237 the same site (Yu et al., 2023). The contribution of coal combustion to ON was higher during nighttime,
238 while the contribution of vehicle emissions was enhanced during rush hours (Figure 2c). Industrial and dust
239 emissions had relatively lower contributions to ON but showed increased contributions during daytime.
240 Unlike many studies reporting biomass burning as a significant source of aerosol ON (Mace et al., 2003;
241 Chen and Chen, 2010; Yu et al., 2017), we found that biomass burning made a negligible contribution to the
242 ON pool in urban Shanghai during our observation period. Note that the observed concentrations of biomass
243 burning markers, including levoglucosan, mannosan, and galactosan, displayed small day-to-day variations
244 (Figure S6). Their upward and downward trends were mainly driven by diel changes, which can be
245 influenced by differences in degradation rates and boundary layer heights between day and night. The
246 contribution of the PMF-resolved biomass burning factor remained relatively constant over the observation
247 period, with only one nighttime peak which might be due to an uncommon nighttime biomass burning event
248 occurred not far from the sampling site (Figure S3). These results indicate absence of influence of notable
249 biomass burning plumes during the entire observation. Consequently, a significant contribution of biomass
250 burning to aerosol ON was not observed. Biomass burning was also a minor contributor (4%) to organic
251 carbon (OC) (Figure S5), similar to previous studies suggesting that biomass burning only contributed 3-4%
252 to OC in urban Shanghai (Li et al., 2020; Huang et al., 2021a). However, levoglucosan showed a good
253 correlation with nitrocatechols (Figure S7), and a significant fraction of ON was associated with



254 nitrocatechol formation processes (Figure 2). This likely indicated that the aging of biomass burning aerosols
255 present in the regional background air produced a number of nitrogen-containing organics, such as
256 nitroaromatic compounds, which contributed significantly to the aerosol ON pool at the urban site. The
257 contribution of primary cooking emissions to ON was generally minor (2%), but it increased to $5\pm 4\%$
258 (ranging from 0.8% to 17%) during dinner time (Figure 2).

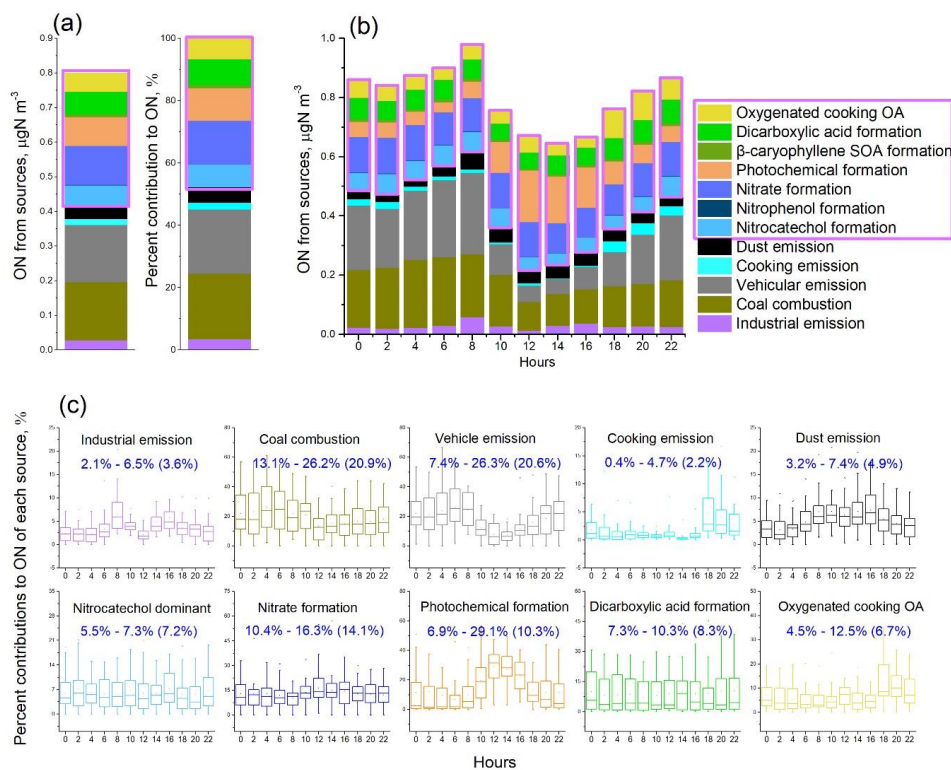
259 Secondary formation processes contributed 48% ($0.38\ \mu\text{gN m}^{-3}$) to ON in the urban atmosphere. Among
260 these processes, a factor related to oxygenated cooking OA was identified through the PMF analysis. This
261 source was characterized by the significant presence of azelaic acid, nonanoic acid, and 9-oxonanoic acid,
262 which are oxidation products of oleic acid or other unsaturated fatty acids with a -C=C at C9 position that
263 are emitted directly from cooking activities (Huang et al., 2021a; Wang et al., 2021). The presence of ON in
264 the oxygenated cooking OA suggests the nitration of primary emitted cooking molecules or oxidation of N-
265 containing molecules of primary cooking emissions (Sugimura et al., 2004; Zhao et al., 2011). Notably, this
266 factor was found to contribute more to aerosol ON than primary cooking emissions. The percent contribution
267 to total ON was 7% during the entire fall-winter observation period and increased to $13\pm 9\%$ during dinner
268 time. When considering both primary cooking emissions and the oxygenated cooking OA, we found a
269 significant contribution (9%) of cooking activities to ON aerosols in urban environments. This contribution
270 was particularly pronounced during dinner time, reaching $17\pm 10\%$. A substantial fraction (14%) of ON was
271 derived from nitrate formation processes, which exhibited minimal diel variation. Photochemical formation
272 processes represented 10% of the ON source, with a significant increase observed from noon to the afternoon.
273 The formation processes of dicarboxylic acids (DCA) and nitrocatechols contributed 8% and 7%,
274 respectively, to the ON budget.

275 ON associated with the factors related to nitrocatechol and nitrophenol formation likely represent the
276 amount of N bound within nitroaromatic compounds, averaging approximately $60\ \text{ngN m}^{-3}$ (Figure 2). This
277 study quantified four nitroaromatic compounds in aerosols, namely 4-nitrophenol, 4-nitrocatechol, 3-methyl-
278 5-nitrocatechol, and 4-methyl-5-nitrocatechol, using the TAG system. The combined N content in the four
279 nitroaromatic compounds averaged at $1.14\ \text{ngN m}^{-3}$, accounting for approximately 2% of the estimated total
280 nitroaromatic-N. In most cases (>90%), the speciated nitroaromatic-N represented less than 10% of total
281 nitroaromatic-N (Figure S8a). Nitroaromatic compounds are known for their significant contributions to
282 aerosol light absorption, and some are recognized as toxicants (Laskin et al., 2015; Zhang et al., 2023). Our
283 findings indicated the substantial presence of the un-speciated mass within this group of N-containing
284 compounds, thus the importance to identify and quantify the unknown nitroaromatics.

285 We estimate the amount of oxidized ON by summing up the ON distributed in the factors related to
286 atmospheric oxidation processes, including the photochemical formation, nitrate formation, and
287 nitroaromatic formation factors. In this way, oxidized ON, mainly organic nitrates and nitroaromatics, had a
288 concentration range of $0.02\text{-}0.85\ \mu\text{gN m}^{-3}$ with an average of $0.25\ \mu\text{gN m}^{-3}$. It accounted for 4-68% (25% on
289 average) of total oxidized N (oxidized ON plus nitrate-N) in the aerosols (Figure S8b). The formation of
290 oxidized ON and inorganic nitrate involves the common precursors of nitrogen oxides (NO_x). Our results
291 suggested the yield of conversion of $\text{NO}_x\text{-N}$ to aerosol ON and nitrate-N has an approximate ratio of 1:3.



292 This estimation, although rough, is valuable for evaluating the fate of NO_x in urban areas. Our analyses
 293 highlight the significance of measuring bulk ON to reveal the abundance of different groups of organic N-
 294 containing aerosols. With comprehensive source markers available, the PMF analysis allows us to apportion
 295 the total aerosol ON mass to different factors (sources), and each fraction of ON may indicate the total
 296 quantity of N from the corresponding sources or formation processes.



297

298 **Figure 2.** PMF source apportionment results for aerosol ON. (a) Overall mass and percent contributions of
 299 resolved sources to aerosol ON during the fall-winter observation period. (b) Diel variations of source
 300 compositions of ON. (c) Diel variation patterns of each ON source. The numerical ranges show the lowest
 301 to highest averages of percent contributions of sources at sampling hours (e.g., 2:00, 4:00). The number in
 302 parentheses are overall percent contributions of sources to ON pool during the observation (i.e., results in
 303 Figure (a)). Contributions of nitrophenol formation and β -caryophyllene SOA formation to ON were very
 304 minor and not shown for their diel variations in (c). Secondary sources of ON are highlighted with a purple
 305 box. The sources of OC can be found in Figure S5.

306

307 3.3 Evidence of formation of reduced ON species

308 It is noteworthy that a significant fraction of ON (8%) was associated with the formation processes of DCAs
 309 (Figure 2). DCAs in ambient aerosols are primarily derived from the oxidation of anthropogenic and biogenic
 310 volatile organic compounds. In this study, the concentration of DCAs increased with rising relative humidity
 311 (RH) (Figure S9), suggesting a higher RH could enhance the aqueous formation of DCAs and/or the gas-to-
 312 particle partitioning of DCAs. The part of ON related to DCA formation processes (here termed as DCA_ON)
 313 may represent the reduced-ON species formed through the heterogenous/aqueous phase reactions between



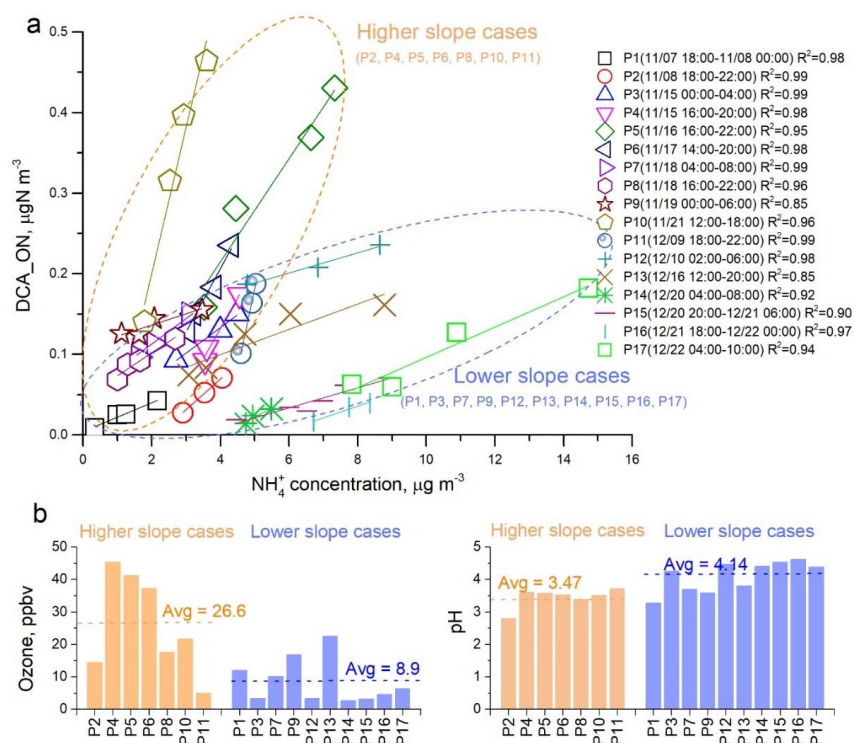
314 DCAs and $\text{NH}_3/\text{NH}_4^+$, as discussed below. Previous lab studies and field measurements have suggested that
315 the amount of particulate NH_4^+ , as measured by AMS, exceeded the quantity required to balance anions
316 including nitrate (NO_3^-), sulfate (SO_4^{2-}), and chloride (Cl^-). The excess NH_4^+ was believed to bind with
317 organic acids such as DCAs to form organic ammonium salts (Schlag et al., 2017; Hao et al., 2020). We note
318 that the measurement of NH_4^+ by AMS relies on the quantification of NH_x^+ fragments, which could also
319 originate from the fragmentation of other reduced ON species, such as amines and amides, in addition to
320 NH_4^+ and organic ammonium salts. Consequently, the specific molecules into which the excess $\text{NH}_4^+\text{-N}$ is
321 incorporated remain unclear due to the lack of molecular information on ON-containing compounds.

322 We examined the relationship between DCA_ON and NH_4^+ concentrations during periods of continuous
323 increment in DCA_ON lasting 4 hours or longer. We identified 17 such cases during the field observation
324 period. Interestingly, DCA_ON showed a strong correlation with NH_4^+ in all these cases (Figure 3a). This
325 result lends support for the hypothesis that DCA_ON may represent reduced ON species formed through the
326 reactions between DCAs and $\text{NH}_3/\text{NH}_4^+$. The slopes of linear regression between DCA_ON and NH_4^+ varied
327 significantly among the cases and could be roughly divided into higher-slope cases and lower-slope cases,
328 with 7 and 10 in these two categories, respectively. (Figure 3a). A higher-slope value indicated a more rapid
329 formation of DCA_ON at a given concentration level of NH_4^+ . The higher-slope cases were distinctly
330 associated with higher O_3 concentration (Figure 3b), suggesting an elevated oxidation capacity and hence
331 enhanced formation of secondary products such as DCAs, which serve as the precursors of DCA_ON.
332 Additionally, the higher-slope cases were associated with lower pH values (higher acidity) as calculated
333 using the thermodynamic equilibrium model ISORROPIA II with MARGA data (Figure 3b). The lower pH
334 facilitated the gas-to-particle partitioning of NH_3 and subsequent reactions involving DCAs and NH_3 . Note
335 that the aqueous formation of imines such as imidazoles through the reactions between carbonyls and
336 $\text{NH}_3/\text{NH}_4^+$ has been established in laboratory studies (Galloway et al., 2009; Noziere et al., 2009) and
337 confirmed by field observations (Zhang et al., 2020; Lian et al., 2021; Liu et al., 2023). Considering the close
338 relationship between carbonyls and DCAs, the possibility that imines contributed to DCA_ON could not be
339 excluded. Overall, these results provided observational evidence of potentially significant formation of
340 reduced ON species through NH_3 chemistry in the real atmosphere.

341 The concentration of DCA_ON had an interquartile range of 8-111 ng N m^{-3} , with an average \pm standard
342 deviation (SD) of $66 \pm 81 \text{ ng N m}^{-3}$ over the observation period. Assuming an average molecular formula of
343 $\text{C}_5\text{H}_7\text{N}_{1.5}\text{O}_{1.5}$ for the reduced-ON species, considering these compounds may contain 3-7 carbon, 1-2
344 nitrogen, and 1-2 oxygen atoms, the concentration of these ON compounds would be 43-592 ng m^{-3} with the
345 average \pm SD being $352 \pm 432 \text{ ng m}^{-3}$. This result provides a rough estimation of the total reduced ON
346 compounds that are formed through $\text{NH}_3/\text{NH}_4^+$ reactions in urban Shanghai. In a recent study conducted in
347 rural Shanghai (Liu et al., 2023), eight imidazoles were detected, and the total concentration of these species
348 ranged from 1.3-15.8 ng m^{-3} (average: $5.5 \pm 3.4 \text{ ng m}^{-3}$). Furthermore, significant increases in imidazole
349 concentrations were observed during humid haze periods, suggesting an aqueous phase formation pathway
350 of these species (Liu et al., 2023). The summed concentration level of the eight imidazoles was lower by 1-
351 2 orders of magnitude compared to our estimated bulk concentration, indicating the prevalence of



352 unidentified reduced ON species. Our analyses suggested that ON aerosols originating from NH₃ chemistry
 353 could be a significant source of nitrogenous SOA. Further investigations are needed to determine their major
 354 chemical compositions and formation mechanisms.
 355



356

357 **Figure 3.** The relationship between ON associated with dicarboxylic acids (DCA) formation (DCA_ON)
 358 and ammonium (NH₄⁺) in the cases that DCA_ON showed continuous increments, and the potential
 359 influence factors. (a) Correlations between DCA_ON and NH₄⁺ concentrations in each of 17 cases where
 360 when DCA_ON exhibited a continuous increment. The cases can be separated into two groups based on their
 361 linear regression slopes, those with higher slopes, enclosed in yellow dashed circles, and those with lower
 362 slopes, enclosed in blue dashed circles. (b) Comparisons of levels of ozone (O₃) and pH in higher slope cases
 363 and lower slope cases.
 364

365 3.4 Factors driving the increment of secondary ON aerosol.

366 The PMF source apportionment analysis has provided the total quantity of the secondary ON (SON) and its
 367 apportionment to individual formation pathways. This greatly facilitates investigating the largely under-
 368 evaluated formation processes of N-containing OA. We next focus on the cases where SON showed
 369 continuous increment for a period of 4 hours or longer and discuss the driving factors behind these
 370 increments. Forty-two cases were identified throughout the entire observation period. To isolate the local
 371 formation of SON from the influence of transported air masses, we extracted cases with wind speeds lower
 372 than 3 m/s as cases of local SON formation (Zhou et al., 2022). The following discussion will exclusively
 373 focus on the local SON formation cases.



374 A total of 24 local SON formation cases were identified and classified into five types based on the
375 dominant formation pathway of SON, as revealed by the PMF analysis. Figure 4 illustrates the variations in
376 the sources of SON and secondary organic carbon (SOC) for the five types of local SON increment. The
377 ensuing discussion shows our paired measurements of bulk aerosol ON and OC, along with subsequent
378 source analyses, provide unique insights into the formation processes of N-containing OA.

379 Type 1 cases, totaling three, were characterized by DCA formation processes driving the increment of SON.
380 In one example of Type 1 case shown in Figure 4, SON increased by $0.33 \mu\text{gN m}^{-3}$ from 16:00-22:00 on
381 November 16. During this period, DCA_ON increased by $0.27 \mu\text{gN m}^{-3}$, accounting for 82% of the variation
382 in SON. Nitrate formation processes also contributed to the SON increment during this period, but to a lesser
383 extent. DCA formation processes were also the dominant source of SOC increase in this case, contributing
384 to the production of $1.05 \mu\text{g C m}^{-3}$ of SOC and 80% of the change in SOC during the period. Note that the
385 atomic ratio of the change in SOC (ΔSOC) to the change in SON (ΔSON) associated with DCA formation
386 processes was 4.5. This ratio indicates that there was approximately 1 nitrogen atom for every 4-5 carbon
387 atoms in the SOA associated with DCA formation processes. The low $\Delta\text{SOC}/\Delta\text{SON}$ ratio suggested the
388 formation of N-containing organic aerosols with low molecular weight and/or multiple N atoms. Considering
389 that some SOA compounds may not contain N atoms, the SON compounds formed through DCA formation
390 processes may have a C/N ratio lower than 4. Possible candidate species include imines, such as methyl- and
391 ethyl-imidazoles, and C2-C5 amides. This result supports the aforementioned hypothesis that DCA_ON
392 likely constitutes of reduced ON species formed through reactions between acids/carbonyls and $\text{NH}_3/\text{NH}_4^+$.
393 All three Types 1 cases occurred during the transition from daytime to nighttime (e.g., from 16:00-22:00).
394 This suggests that acids/carbonyls accumulated during the daytime through photochemical processes and
395 then entered the aqueous phase during nighttime, where they reacted with $\text{NH}_3/\text{NH}_4^+$ to form reduced ON
396 species under higher air humidity.

397 Type 2 cases, totaling seven, featured photochemical formation as the dominant source driving SON
398 increment. They mostly occurred during the morning to noon periods, suggesting formation of SON through
399 photochemical processes. In the Type 2 case presented in Figure 4, ΔSON was $0.18 \mu\text{gN m}^{-3}$ and ΔSOC was
400 $0.97 \mu\text{g C m}^{-3}$. Photochemical formation contributed $0.1 \mu\text{gN m}^{-3}$ of SON and $0.61 \mu\text{g C m}^{-3}$ of SOC, yielding
401 a $\Delta\text{SOC}/\Delta\text{SON}$ atomic ratio of 7.1. This result suggested significant formation of N-containing organic
402 molecules with a C/N ratio of 6-8. Examples of such species include nitroaromatic compounds and organic
403 nitrates. The frequent occurrence of Type 2 cases suggested an efficient formation of oxidized ON species
404 in urban areas.

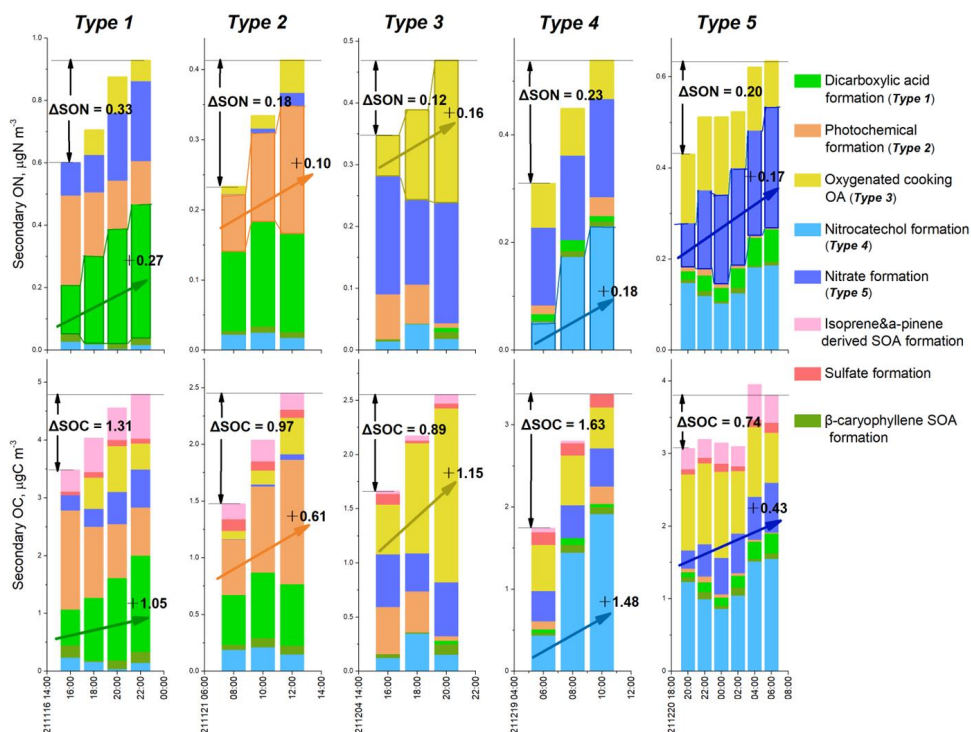
405 Type 3 cases, totaling six, exhibit SON increase driven by oxidation of cooking emissions. Their
406 occurrences coincided with lunch and dinner hours. Take the case during 16:00-20:00 of December 4 as an
407 example, $0.16 \mu\text{gN m}^{-3}$ of ΔSON and $1.15 \mu\text{g C m}^{-3}$ of ΔSOC were formed, resulting in a C/N ratio of 8.4
408 for the SOA associated with the cooking emission oxidation. Chamber simulations have shown that SOA
409 produced through oxidation of cooking fumes can be more abundant than primary OA species from cooking
410 emissions (Liu et al., 2018b). However, the chemical compositions and underlying formation mechanisms
411 of N-containing organic aerosols remain uncertain. This study, for the first time, reveals the potentially



412 significant contribution of cooking oxidation to N-containing SOA in the real urban atmosphere. Future
413 efforts are recommended to direct towards investigating representative N-containing molecules formed
414 through cooking oxidation and their formation pathways.

415 Four Type 4 cases were identified, each characterized by the dominant contribution of nitrocatechol
416 formation to ON increase and all occurred during the daytime. Take the case between 06:00 and 10:00 on
417 December 19 as an example, the sum concentration of 4-nitrocatechol, 3-methyl-5-nitrocatechol, and 4-
418 methyl-5-nitrocatechol (Table S1) rose from 9.52 to 24.64 ng m⁻³. This increase was attributed to secondary
419 formation processes of nitroaromatic compounds, instead of primary emissions, as evidenced by the flat or
420 decreasing trends of elemental carbon (EC) and nitric oxide (NO) during that period (Figure S10). The
421 increment in SON and SOC associated with the nitrocatechol formation factor was 0.18 µgN m⁻³ and 1.48
422 µgC m⁻³, respectively over the four-hour period (Figure 4), resulting in a ΔSOC/ΔSON atomic ratio of 9.6.
423 This portion of SON may represent the N content in nitroaromatic compounds formed through processes
424 analogous to nitrocatechol formation.

425 Four Type 5 cases were identified, each characterized with nitrate formation processing as the driving
426 source for the increase in SON. This fraction of SON may indicate the formation of organic nitrates, which
427 share common precursor of NO_x with nitrate. Organic nitrates have long been recognized as significant
428 components of secondary organic aerosols in ambient air (Rollins et al., 2012; Perring et al., 2013). Organic
429 nitrate formation encompasses two main pathways: hydroxyl radical (OH)-initiated oxidation of
430 hydrocarbons in the presence of NO_x during the day and nitrate radical (NO₃)-initiated oxidation of alkenes
431 during the night. Both pathways involve the formation of organic nitrates in the gas phase, followed by
432 partitioning to the particulate phase (Perring et al., 2013). This study, through integrated analyses of SON
433 and SOC, provides evidence suggesting that organic nitrates might also form through heterogeneous or
434 aqueous reactions. As depicted in Figure 4, the nitrate formation process produced 0.17 µgN m⁻³ of ΔSON
435 and 0.43 µg C m⁻³ of ΔSOC from the night of December 20 to the following morning, yielding a
436 ΔSOC/ΔSON atomic ratio of only 2.9. Gas-phase formation of organic nitrates followed by gas-to-particle
437 partitioning would not result in such a low C/N ratio. Therefore, a significant number of organic nitrates
438 might be formed through heterogeneous or aqueous reactions between organic compounds and HNO₃/NO₃,
439 enhancing the ON content while not affecting the OC content which is already present in the particle phase.
440 In a previous study, it was suggested that organic nitrates can be produced through non-radical reactions of
441 hydrated glyoxal and nitric acid in the aqueous phase (Lim et al., 2016). Xu et al. (2020) found that aerosol
442 liquid water promotes the formation of water-soluble ON, likely in the form of organic nitrate species.
443 Previous studies have identified an 80% underestimation of monoterpene hydroxyl nitrate by the GEOS-
444 Chem model, which considers both OH oxidation and NO₃ oxidation mechanisms of monoterpene (Li et al.,
445 2018; Zhang et al., 2021), indicating an incomplete understanding of the formation mechanisms of organic
446 nitrates. Our observational results, combined with previous investigations, suggest the need for further
447 exploration of the formation mechanisms of particulate organic nitrates, such as heterogeneous/aqueous
448 phase reaction processes.



449

450 **Figure 4.** Five types of SON increment were driven by different formation processes. The increment amounts of SON (Δ SON) and SOC (Δ SOC) in each type are shown. The dominant formation processes of ON and
 451 of SON (Δ SON) and SOC (Δ SOC) in each type are shown. The dominant formation processes of ON and
 452 of SON (Δ SON) and SOC (Δ SOC) in each type are shown. The dominant formation processes of ON and
 453 of SON (Δ SON) and SOC (Δ SOC) in each type are shown. The dominant formation processes of ON and

454 4 Conclusion and implications

455 Presently, the knowledge of total aerosol ON budget is severely limited, with source analysis predominantly
 456 qualitative. Building on a methodological breakthrough that allows for the online measurement of bulk
 457 aerosol ON and concurrent measurements of a comprehensive array of molecular source tracers, we have
 458 identified both primary emissions and secondary formation processes as substantial contributors to PM_{2.5}
 459 ON mass in urban Shanghai during the fall-winter period of 2021. While we acknowledge uncertainties of
 460 PMF modeling in apportioning sources to bulk ON, this approach facilitates identification of major
 461 sources/formation processes and provides quantitative insight into the relative importances.

462 The observed dominance of primary ON sources such as coal combustion and vehicle emissions, alongside
 463 the significant contributions from secondary formation processes like nitrate formation, photochemical
 464 processes, and DCA formation, indicates the multi-faceted nature of ON aerosol production in urban
 465 environments. The identification of specific secondary formation pathways, including nitroaromatics
 466 formation, DCA formation, and oxygenated cooking OA, sheds light on the diverse precursors and chemical
 467 processes involved in aerosol formation and evolution. Notably, we have provided valuable observational
 468 evidence on secondary ON aerosol formation through NH₃ and NO_x chemistries, the joint evaluation of



469 which has been under-explored in the past.

470 The quantification of ON contributions from various sources and the elucidation of secondary formation
471 mechanisms provide a basis for targeted mitigation strategies aimed at reducing ON emissions and
472 improving air quality in urban areas. The insights gained from this study can inform policy decisions and
473 regulatory measures to curb primary emission sources and mitigate the impact of secondary formation
474 processes on ON aerosol levels.

475 Looking ahead, future research efforts should focus on refining our understanding of the detailed
476 mechanisms driving ON aerosol formation, including the chemical reactions involving major precursors and
477 secondary processes. Furthermore, continued monitoring and analysis of ON aerosol composition in
478 different environmental settings will be crucial for assessing the broader implications of ON aerosols on air
479 quality, climate, and public health. Bulk ON measurements enable mass closure and are advantageous for
480 constraining the major sources and formation processes of ON aerosols. This methodology complements the
481 molecular-level characterization of ON molecules, which provides chemical composition information but
482 falls short on capturing total ON. Future research efforts should emphasize identifying and quantifying ON
483 species that can indicate specific sources and formation processes.

484

485 **Financial support.** This work was supported by Science and Technology Commission of Shanghai
486 Municipality (20dz1204000), the Research Grants Council of Hong Kong (16213222 and 16304519).

487

488 **Author contributions.** XY and JZY conceived the research, designed the research plan and wrote the
489 manuscript; XY, MZ, SHZ, LPQ, JLL, YGM and HLW carried out the instrumental measurements; XY, ZJZ,
490 and KZL carried out data analysis.

491

492 **Competing interests.** The contact author has declared that none of the authors has any competing interests.

493

494 **Data availability.** Data used in this study is available upon request from the corresponding author.

495

496 REFERENCES

- 497 Andersen, K. M., Mayor, J. R., and Turner, B. L.: Plasticity in N uptake among sympatric species with contrasting
498 nutrient acquisition strategies in a tropical forest, *Ecology*, 98, 1388-1398, 2017.
- 499 Bandowe, B. A. M. and Meusel, H.: Nitrated polycyclic aromatic hydrocarbons (nitro-PAHs) in the environment
500 - A review, *Sci. Total Environ.*, 581-582, 237-257, 2017.
- 501 Bones, D. L., Henricksen, D. K., Mang, S. A., Gonsior, M., Bateman, A. P., Nguyen, T. B., Cooper, W. J., and
502 Nizkorodov, S. A.: Appearance of strong absorbers and fluorophores in limonene-O₃ secondary organic aerosol
503 due to NH₄⁺-mediated chemical aging over long time scales, *J. Geophys. Res.-Atmos.*, 115, D05203,
504 doi:10.1029/2009JD012864, 2010.
- 505 Cape, J. N., Cornell, S. E., Jickells, T. D., and Nemitz, E.: Organic nitrogen in the atmosphere — Where does it
506 come from? A review of sources and methods, *Atmos. Res.*, 102, 30-48, 2011.
- 507 Chen, H. Y. and Chen, L. D.: Occurrence of water soluble organic nitrogen in aerosols at a coastal area, *J. Atmos.*
508 *Chem.*, 65, 49-71, 2010.
- 509 Chow, K. S., Huang, X. H. H., and Yu, J. Z.: Quantification of nitroaromatic compounds in atmospheric fine
510 particulate matter in Hong Kong over 3 years: field measurement evidence for secondary formation derived
511 from biomass burning emissions, *Environ. Chem.*, 13, 665-673, 2016.
- 512 Duan, F. K., Liu, X. D., He, K. B., and Dong, S. P.: Measurements and characteristics of nitrogen-containing



- 513 compounds in atmospheric particulate matter in Beijing, China, *Bull. Environ. Contam. Toxicol.*, 82, 332–337,
514 2009.
- 515 Farmer, D. K., Matsunaga, A., Docherty, K. S., Surratt, J. D., Seinfeld, J. H., Ziemann, P. J., and Jimenez, J. L.:
516 Response of an aerosol mass spectrometer to organonitrates and organosulfates and implications for
517 atmospheric chemistry, *Proc. Natl. Acad. Sci. U. S. A.*, 107, 6670–6675, 2010.
- 518 Galloway, M. M., Chhabra, P. S., Chan, A. W. H., Surratt, J. D., Flagan, R. C., Seinfeld, J. H., and Keutsch, F. N.:
519 Glyoxal uptake on ammonium sulphate seed aerosol: reaction products and reversibility of uptake under dark
520 and irradiated conditions, *Atmos. Chem. Phys.*, 9, 3331–3345, 2009.
- 521 Hao, L. Q., Kari, E., Leskinen, A., Worsnop, D. R., and Virtanen, A.: Direct contribution of ammonia to α -pinene
522 secondary organic aerosol formation, *Atmos. Chem. Phys.*, 20, 14393–14405, 2020.
- 523 He, X., Wang, Q. Q., Huang, X. H. H., Huang, D. D., Zhou, M., Qiao, L. P., Zhu, S. H., Ma, Y. G., Wang, H. L.,
524 Li, L., Huang, C., Xu, W., Worsnop, D. R., Goldstein, A. H., and Yu, J. Z.: Hourly measurements of organic
525 molecular markers in urban Shanghai, China: Observation of enhanced formation of secondary organic aerosol
526 during particulate matter episodic periods, *Atmos. Environ.*, 240, 117807, 2020.
- 527 Ho, K. F., Ho, S. S. H., Huang, R. J., Chuang, H. C., Cao, J. J., Han, Y. M., Lui, K. H., Ning, Z., Chuang, K. J.,
528 Cheng, T. J., Lee, S. C., Hu, D., Wang, B., and Zhang, R. J.: Chemical composition and bioreactivity of PM_{2.5}
529 during 2013 haze events in China, *Atmos. Environ.*, 126, 162–170, 2016.
- 530 Huang, D. D., Zhu, S. H., An, J. Y., Wang, Q. Q., Qiao, L. P., Zhou, M., He, X., Ma, Y. G., Sun, Y. L., Huang, C.,
531 Yu, J. Z., and Zhang, Q.: Comparative Assessment of Cooking Emission Contributions to Urban Organic
532 Aerosol Using Online Molecular Tracers and Aerosol Mass Spectrometry Measurements, *Environ. Sci.*
533 *Technol.*, 55, 14526–14535, 2021a.
- 534 Huang, W., Yang, Y., Wang, Y. H., Gao, W. K., Li, H. Y., Zhang, Y. Y., Li, J. Y., Zhao, S. M., Yan, Y. C., Ji, D. S.,
535 Tang, G. Q., Liu, Z. R., Wang, L. L., Zhang, R. J., and Wang, Y. S.: Exploring the inorganic and organic nitrate
536 aerosol formation regimes at a suburban site on the North China Plain, *Sci. Total Environ.*, 768, 144538,
537 10.1016/j.scitotenv.2020.144538, 2021b.
- 538 Jickells, T., Baker, A. R., Cape, J. N., Cornell, S. E., and Nemitz, E.: The cycling of organic nitrogen through the
539 atmosphere, *Philos Trans R Soc Lond B Biol Sci*, 368, 20130115, 2013.
- 540 Kielland, K., McFarland, J. W., and Olson, K.: Amino acid uptake in deciduous and coniferous taiga ecosystems,
541 *Plant Soil*, 288, 297–307, 2006.
- 542 Laskin, A., Laskin, J., and Nizkorodov, S. A.: Chemistry of Atmospheric Brown Carbon, *Chem. Rev.*, 115,
543 4335–4382, 2015.
- 544 Li, R., Wang, Q. Q., He, X., Zhu, S. H., Zhang, K., Duan, Y. S., Fu, Q. Y., Qiao, L. P., Wang, Y. J., Huang, L., Li,
545 L., and Yu, J. Z.: Source apportionment of PM_{2.5} in Shanghai based on hourly organic molecular markers and
546 other source tracers, *Atmos. Chem. Phys.*, 20, 12047–12061, 2020.
- 547 Li, R., Wang, X. F., Gu, R. R., Lu, C. Y., Zhu, F. P., Xue, L. K., Xie, H. J., Du, L., Chen, J. M., and Wang, W. X.:
548 Identification and semi-quantification of biogenic organic nitrates in ambient particulate matters by
549 UHPLC/ESI-MS, *Atmos. Environ.*, 176, 140–147, 2018.
- 550 Li, Y. M., Fu, T. M., Yu, J. Z., Yu, X., Chen, Q., Miao, R. Q., Zhou, Y., Zhang, A. X., Ye, J. H., Yang, X., Tao, S.,
551 Liu, H. B., and Yao, W. Q.: Dissecting the contributions of organic nitrogen aerosols to global atmospheric
552 nitrogen deposition and implications for ecosystems, *Natl. Sci. Rev.*, 10, nwad244, 2023.
- 553 Li, Z. J., Nizkorodov, S. A., Chen, H., Lu, X. H., Yang, X., and Chen, J. M.: Nitrogen-containing secondary organic
554 aerosol formation by acrolein reaction with ammonia/ammonium, *Atmos. Chem. Phys.*, 19, 1343–1356, 2019.
- 555 Lian, X. F., Zhang, G. H., Yang, Y. X., Lin, Q. H., Fu, Y. Z., Jiang, F., Peng, L., Hu, X. D., Chen, D. H., Wang, X.
556 M., Peng, P. A., Sheng, G. Y., and Bi, X. H.: Evidence for the Formation of Imidazole from Carbonyls and
557 Reduced Nitrogen Species at the Individual Particle Level in the Ambient Atmosphere, *Environ. Sci. Technol.*
558 *Lett.*, 8, 9–15, 2021.
- 559 Lim, Y. B., Kim, H., Kim, J. Y., and Turpin, B. J.: Photochemical organonitrate formation in wet aerosols, *Atmos.*
560 *Chem. Phys.*, 16, 12631–12647, 2016.
- 561 Liu, F. X., Bi, X. H., Zhang, G. H., Lian, X. F., Fu, Y. Z., Yang, Y. X., Lin, Q. H., Jiang, F., Wang, X. M., Peng, P.
562 A., and Sheng, G. Y.: Gas-to-particle partitioning of atmospheric amines observed at a mountain site in southern
563 China, *Atmos. Environ.*, 195, 1–11, 2018a.
- 564 Liu, T. Y., Wang, Z., Huang, D. D., Wang, X. M., and Chan, C. K.: Significant Production of Secondary Organic
565 Aerosol from Emissions of Heated Cooking Oils, *Environ. Sci. Technol. Lett.*, 5, 32–37, 2018b.
- 566 Liu, X. D., Wang, H. Y., Wang, F. L., Lv, S. J., Wu, C., Zhao, Y., Zhang, S., Liu, S. J., Xu, X. B., Lei, Y. L., and
567 Wang, G. H.: Secondary Formation of Atmospheric Brown Carbon in China Haze: Implication for an Enhancing
568 Role of Ammonia, *Environ. Sci. Technol.*, 57, 11163–11172, 2023.
- 569 Mace, K. A., Artaxo, P., and Duce, R. A.: Water-soluble organic nitrogen in Amazon Basin aerosols during the dry
570 (biomass burning) and wet seasons, *J. Geophys. Res.*, 108, doi:10.1029/2003JD003557, 2003a.
- 571 Matsumoto, K., Sakata, K., and Watanabe, Y.: Water-soluble and water-insoluble organic nitrogen in the dry and
572 wet deposition, *Atmos. Environ.*, 218, doi.org/10.1016/j.atmosenv.2019.117022, 2019.



- 573 Miller-Schulze, J. P., Paulsen, M., Toriba, A., Tang, N., Hayakawa, K., Tamura, K., Dong, L. J., Zhang, X. M.,
574 and Simpson, C. D.: Exposures to Particulate Air Pollution and Nitro-Polycyclic Aromatic Hydrocarbons
575 among Taxi Drivers in Shenyang, China, *Environ. Sci. Technol.*, 44, 216-221, 2010.
- 576 Miyazaki, Y., Kawamura, K., Jung, J., Furutani, H., and Uematsu, M.: Latitudinal distributions of organic nitrogen
577 and organic carbon in marine aerosols over the western North Pacific, *Atmos. Chem. Phys.*, 11 (7), 3037-3049,
578 2011.
- 579 Nakamura, T., Ogawa, H., Maripi, D. K., and Uematsu, M.: Contribution of water soluble organic nitrogen to total
580 nitrogen in marine aerosols over the East China Sea and western North Pacific, *Atmos. Environ.*, 40, 7259–
581 7264, 2006.
- 582 Noziere, B., Dziedzic, P., and Cordova, A.: Products and kinetics of the liquid-phase reaction of glyoxal catalyzed
583 by ammonium ions (NH_4^+), *J. Phys. Chem. A*, 113, 231–237, 2009.
- 584 Pavuluri, C. M., Kawamura, K., and Fu, P. Q.: Atmospheric chemistry of nitrogenous aerosols in northeastern
585 Asia: biological sources and secondary formation, *Atmos. Chem. Phys.*, 15 (17), 9883-9896, 2015.
- 586 Perring, A. E., Pusede, S. E., and Cohen, R. C.: An observational perspective on the atmospheric impacts of alkyl
587 and multifunctional nitrates on ozone and secondary organic aerosol, *Chem. Rev.*, 113, 5848–5870, 2013.
- 588 Qiao, L. P., Cai, J., Wang, H. L., Wang, W. B., Zhou, M., Lou, S. R., Chen, R. J., Dai, H. X., Chen, C. H., and Kan,
589 H. D.: $\text{PM}_{2.5}$ constituents and hospital emergency-room visits in Shanghai, China, *Environ. Sci. Technol.*,
590 48(17), 10,406–10,414, 2014.
- 591 Qiu, C., Wang, L., Lal, V., Khalizov, A. F., and Zhang, R. Y.: Heterogeneous Reactions of Alkylamines with
592 Ammonium Sulfate and Ammonium Bisulfate, *Environ. Sci. Technol.*, 45, 4748–4755, 2011.
- 593 Ren, L. J., Bai, H. H., Yu, X., Wu, F. C., Yue, S. Y., Ren, H., Li, L. J., Lai, S. C., Sun, Y. L., Wang, Z. F., and Fu,
594 P. Q.: Molecular composition and seasonal variation of amino acids in urban aerosols from Beijing, China,
595 *Atmos. Res.*, 203, 28–35, 2018.
- 596 Rizwan Khan, M., Naushad, M., and Abdullah Alothman, Z.: Presence of heterocyclic amine carcinogens in home-
597 cooked and fast-food camel meat burgers commonly consumed in Saudi Arabia, *Sci. Rep.*, 7, 1707,
598 doi:10.1038/s41598-017-01968-x, 2017.
- 599 Rollins, A. W., Browne, E. C., Min, K. E., Pusede, S. E., Wooldridge, P. J., Gentner, D. R., Goldstein, A. H., Liu,
600 S., Day, D. A., Russell, L. M., and Cohen, R. C.: Evidence for NO_x Control over Nighttime SOA Formation,
601 *Science*, 337, 1210–1212, 2012.
- 602 Samy, S. and Hays, M. D.: Quantitative LC-MS for water-soluble heterocyclic amines in fine aerosols ($\text{PM}_{2.5}$) at
603 Duke Forest, USA, *Atmos. Environ.*, 72, 77-80, 2013.
- 604 Schlag, P., Rubach, F., Mentel, T. F., Reimer, D., Canonaco, F., Henzing, J. S., Moerman, M., Otjes, R., Prevot, A.
605 S. H., Rohrer, F., Rosati, B., Tillmann, R., Weingartner, E., and Kiendler-Scharr, A.: Ambient and laboratory
606 observations of organic ammonium salts in PM_{10} , *Faraday Discuss.*, 200, 331, 2017.
- 607 Sugimura, T., Wakabayashi, K., Nakagama, H., and Nagao, M.: Heterocyclic amines: Mutagens/carcinogens
608 produced during cooking of meat and fish, *Cancer Sci.*, 95, 290–299, 2004.
- 609 Violaki, K. and Mihalopoulos, N.: Urea: An important piece of Water Soluble Organic Nitrogen (WSON) over
610 the Eastern Mediterranean, *Sci. Total Environ.*, 409, 4796–4801, 2011.
- 611 Violaki, K. and Mihalopoulos, N.: Water-soluble organic nitrogen (WSON) in size-segregated atmospheric
612 particles over the Eastern Mediterranean, *Atmos. Environ.*, 44, 4339-4345, 2010.
- 613 Wang, Q. Q. and Yu, J. Z.: Ambient Measurements of Heterogeneous Ozone Oxidation Rates of Oleic, Elaidic,
614 and Linoleic Acid Using a Relative Rate Constant Approach in an Urban Environment, *Geophys. Res. Lett.*, 48,
615 e2021GL095130, 2021.
- 616 Wang, Q. Q., Huang, X. H. H., Zhang, T., Zhang, Q. Y., Feng, Y. M., Yuan, Z. B., Wu, D., Lau, A. K. H., and Yu,
617 J. Z.: Organic tracer-based source analysis of $\text{PM}_{2.5}$ organic and elemental carbon: A case study at Dongguan
618 in the Pearl River Delta, China, *Atmos. Environ.*, 118, 164-175, 2015.
- 619 Wang, Q. Q., Qiao, L. P., Zhou, M., Zhu, S. H., Griffith, S., Li, L., and Yu, J. Z.: Source apportionment of $\text{PM}_{2.5}$
620 using hourly measurements of elemental tracers and major constituents in an urban environment: Investigation
621 of time-resolution influence, *J. Geophys. Res. Atmos.*, 123, 5284–5300, 2018.
- 622 Wei, S. L., Huang, B., Liu, M., Bi, X. H., Ren, Z. F., Sheng, G. Y., and Fu, J. M.: Characterization of $\text{PM}_{2.5}$ -bound
623 nitrated and oxygenated PAHs in two industrial sites of South China, *Atmos. Res.*, 109–110, 76–83, 2012.
- 624 Williams, B. J., Goldstein, A. H., Kreisberg, N. M., and Hering, S. V.: An in-situ instrument for speciated organic
625 composition of atmospheric aerosols: thermal Desorption Aerosol GC/MS-FID (TAG), *Aerosol Sci. Technol.*,
626 40, 627–638, 2006.
- 627 Xie, M., Chen, X., Hays, M. D., Lewandowski, M., Offenberg, J., Kleindienst, T. E., and Holder, A. L.: Light
628 absorption of secondary organic aerosol: composition and contribution of nitroaromatic compounds, *Environ.*
629 *Sci. Technol.*, 51(20), 11607-11616, 2017.
- 630 Xu, W. Q., Takeuchi, M., Chen, C., Qiu, Y. M., Xie, C. H., Xu, W. Y., Ma, N., Worsnop, D. R., Ng, N. L., and Sun,
631 Y. L.: Estimation of particulate organic nitrates from thermodesorber-aerosol mass spectrometer measurements
632 in the North China Plain, *Atmos. Meas. Tech.*, 14, 3693–3705, 2021.



- 633 Xu, Y., Miyazaki, Y., Tachibana, E., Sato, K., Ramasamy, S., Mochizuki, T., Sadanaga, Y., Nakashima, Y.,
634 Sakamoto, Y., Matsuda, K., and Kajii, Y.: Aerosol Liquid Water Promotes the Formation of Water-Soluble
635 Organic Nitrogen in Submicrometer Aerosols in a Suburban Forest, *Environ. Sci. Technol.*, 54, 1406–1414,
636 2020.
- 637 Yao, L., Garmash, O., Bianchi, F., Zheng, J., Yan, C., Kontkanen, J., Junninen, H., Mazon, S. B., Ehn, M.,
638 Paasonen, P., Sipila, M., Wang, M. Y., Wang, X. K., Xiao, S., Chen, H. F., Lu, Y. Q., Zhang, B. W., Wang, D.
639 F., Fu, Q. Y., Geng, F. H., Li, L., Wang, H. L., Qiao, L. P., Yang, X., Chen, J. M., Kerminen, V., Petäjä, T.,
640 Worsnop, D. R., Kulmala, M., and Wang, L.: Atmospheric new particle formation from sulfuric acid and amines
641 in a Chinese megacity, *Science*, 361, 278–281, 2018.
- 642 Yu, X., Li, Q. F., Ge, Y., Li, Y. M., Liao, K. Z., Huang, X. H. H., Li, J. J., and Yu, J. Z.: Simultaneous Determination
643 of Aerosol Inorganic and Organic Nitrogen by Thermal Evolution and Chemiluminescence Detection, *Environ.*
644 *Sci. Technol.*, 55, 11579–11589, 2021.
- 645 Yu, X., Li, Q. F., Liao, K. Z., Li, Y. M., Wang, X. M., Zhou, Y., Liang, Y. M., and Yu, J. Z.: New measurements
646 reveal a large contribution of nitrogenous molecules to ambient organic aerosol, *npj Clim. Atmos. Sci.*, 7, 72,
647 <https://doi.org/10.1038/s41612-024-00620-6>, 2024.
- 648 Yu, X., Yu, Q. Q., Zhu, M., Tang, M. J., Li, S., Yang, W. Q., Zhang, Y. L., Deng, W., Li, G. H., Yu, Y. G., Huang,
649 Z. H., Song, W., Ding, X., Hu, Q. H., Li, J., Bi, X. H., and Wang, X. M.: Water Soluble Organic Nitrogen
650 (WSO) in Ambient Fine Particles Over a Megacity in South China: Spatiotemporal Variations and Source
651 Apportionment, *J. Geophys. Res. Atmos.*, 122, 13,045–13,060, 2017.
- 652 Yu, X., Zhou, M., Li, J. J., Qiao, L. P., Lou, S. R., Han, W. Y., Zhang, Z. J., Huang, C., and Yu, J. Z.: First Online
653 Observation of Aerosol Total Organic Nitrogen at an Urban Site: Insights Into the Emission Sources and
654 Formation Pathways of Nitrogenous Organic Aerosols, *J. Geophys. Res. Atmos.*, 128, e2023JD038921, 2023.
- 655 Zhang, G. H., Lian, X. F., Fu, Y. Z., Lin, Q. H., Li, L., Song, W., Wang, Z. Y., Tang, M. J., Chen, D. H., Bi, X. H.,
656 Wang, X. M., and Sheng, G. Y.: High secondary formation of nitrogen-containing organics (NOCs) and its
657 possible link to oxidized organics and ammonium, *Atmos. Chem. Phys.*, 20, 1469–1481, 2020.
- 658 Zhang, J., Wang, X.F., Li, R., Dong, S.W., Chen, J., Zhang, Y.N., Zheng, P.G., Li, M., Chen, T.S., Liu, Y.H.,
659 Xue, L.K., Zhou, X.H., Du, L., Zhang, Q.Z., and Wang, W.X.: Significant impacts of anthropogenic activities
660 on monoterpene and oleic acid-derived particulate organic nitrates in the North China Plain, *Atmos. Res.*, 408,
661 256, 2021.
- 662 Zhang, Q. Y., Ma, H. M., Li, J., Jiang, H. X., Chen, W. J., Wan, C., Jiang, B., Dong, G. H., Zeng, X. W., Chen, D.
663 H., Lu, S. Y., You, J., Yu, Z. Q., Wang, X. M., and Zhang, G.: Nitroaromatic Compounds from Secondary Nitrate
664 Formation and Biomass Burning Are Major Proinflammatory Components in Organic Aerosols in Guangzhou:
665 A Bioassay Combining High-Resolution Mass Spectrometry Analysis, *Environ. Sci. Technol.*, 57, 21570–
666 21580, 2023.
- 667 Zhang, Q., Anastasio, C., and Jimenez-Cruz, M.: Water-soluble organic nitrogen in atmospheric fine particles
668 (PM_{2.5}) from northern California, *J. Geophys. Res.*, 107, D11, 4112, [10.1029/2001JD000870](https://doi.org/10.1029/2001JD000870), 2002.
- 669 Zhao, Z. J., Husainy, S., Stoudemayer, C. T., and Smith, G. D.: Reactive uptake of NO₃ radicals by unsaturated
670 fatty acid particles, *Phys. Chem. Chem. Phys.*, 13, 17809–17817, 2011.
- 671 Zhou, M., Nie, W., Qiao, L. P., Huang, D. D., Zhu, S. H., Lou, S. R., Wang, H. L., Wang, Q., Tao S. K., Sun, P.,
672 Liu, Y. W., Xu, Z., An, J. Y., Yan, R. S., Huang, C., Ding, A. J., and Chen, C. H.: Elevated Formation of
673 Particulate Nitrate From N₂O₅ Hydrolysis in the Yangtze River Delta Region From 2011 to 2019, *Geophys. Res.*
674 *Lett.*, 49, e2021GL097393, 2022.
- 675 Zhu, S. H., Wang, Q. Q., Qiao, L. P., Zhou, M., Wang, S., Lou, S. R., Huang, D. D., Wang, Q., Jing, S. G., Wang,
676 H. L., Chen, C. H., Huang, C., and Yu, J. Z.: Tracer-based Characterization of Source Variations of PM_{2.5} and
677 Organic Carbon in Shanghai Influenced by the COVID-19 Lockdown, *Faraday Discuss.*, 226, 112–137, 2021.